O-mediated layer growth of Cu on Ru(0001)



1999 J. Phys.: Condens. Matter 11 19

(http://iopscience.iop.org/0953-8984/11/1/003)

J. Phys.: Condens. Matter **11** (1999) 19–37. Printed in the UK PII: S0953-8984(99)96281-1

# O-mediated layer growth of Cu on Ru(0001)

H Wolter†, K Meinel†, Ch Ammer†, K Wandelt‡ and H Neddermeyer†

† Martin-Luther-Universität Halle-Wittenberg, Fachbereich Physik, D-06099 Halle, Germany
‡ Universität Bonn, Institut für Physikalische und Theoretische Chemie, D-53115 Bonn, Germany

Received 27 July 1998

**Abstract.** The film growth of Cu on clean and O-precovered Ru(0001) at different growth temperatures form 300 K to 450 K was investigated by scanning tunnelling microscopy (STM). Cu films on clean Ru(0001) grow in a multilayer mode at these temperatures. By using an O precoverage ($\Theta_O$) in the range of 0.1 monolayers (ML) up to a saturation coverage of 0.5 ML on clean Ru(0001), at 400 K different growth regimes are obtained. For $\Theta_O < 0.2$ ML a multilayer mode is preserved which changes into an O-induced two-dimensional (2D) growth for higher $\Theta_O$ (0.2–0.5 ML). STM reveals the formation of an O/Cu surfactant structure on the surface due to migration of O initially located at the Ru surface. Its surface coverage rises linearly with O precoverage up to $\Theta_O = 0.4$ ML where it covers the surface completely. By increasing $\Theta_O$ up to 0.5 ML, a drastic change in the morphology and density of the 2D islands occurs, which is accompanied by a change of the O/Cu surfactant structure. The O/Cu surfactant structure displays some order on a local scale for low $\Theta_O$, which changes into a disordered structure for $\Theta_O > 0.4$ ML. Structural similarities to oxidized surfaces of Cu(111) and the structures induced by $O_2$ postadsorption on Cu/Ru(0001) are discussed. Different models of surfactant mechanisms are presented to explain the observations. The locally ordered O/Cu surfactant structure (for $\Theta_O < 0.4$ ML) together with specific Cu film defects induce a heterogeneous nucleation of Cu with a high island density. Different mobilities of migrating Cu adatoms are established on top of the small islands and on the O/Cu structure resulting in enhanced interlayer diffusion explaining the observed 2D growth. The average island density only slightly changes within the temperatures investigated. In contrast, the saturated and disordered O/Cu surfactant structure (for $\Theta_O = 0.4$–0.5 ML) causes homogeneous nucleation. For this structure, the island density strongly depends on temperature and gives rise to an Arrhenius-like behaviour. The observed 2D growth is attributed to a reduction of the interlayer diffusion barrier. Cu growth on a formerly annealed Cu/O/Ru(0001) film system yields an almost perfect layer-by-layer growth caused by heterogeneous nucleation at periodically arranged Cu film defect sites. The relationship of the O/Cu surfactant structures to the ordered $(3 \times 2\sqrt{3})$ O/Cu bilayer on Ru(0001)—interpreted as a disrupted $Cu_2O$-like oxidized surface—was revealed.

## 1. Introduction

A defined layer-by-layer growth of epitaxial films is of great importance for industrial production techniques such as that of semiconductor devices, reactive surface and sensors. Small amounts of foreign material known as surfactants play an active role in film formation. The knowledge of the basic surfactant effects on an atomic scale offer the possibility of deliberately controlling the growth processes of various material/substrate combinations by using a suitable surfactant. The growth of a thin film is normally defined by kinetic processes rather than by thermodynamical equilibrium of the system. The growth proceeds by a sequence of nucleation, island growth and coalescence. The migrating adatoms either form stable nuclei on terraces or are captured by steps. After reaching the saturation density, the nuclei grow into two-dimensional (2D) islands which expand and coalesce. To maintain a 2D growth,

  

it is necessary that adatoms impinging on top of the islands migrate over the step edge. If nucleation starts on the islands before they coalesce, a three-dimensional (3D) growth results. The decisive parameter for the growth mode is the interlayer diffusion over the step edge which is controlled by an additional energy barrier [1, 2] with respect to the diffusion barriers on terraces. To change a 3D growth into layer growth, the interlayer diffusion has to be intensified by either reducing the additional step edge energy barrier directly or by inducing a higher mobility of adatoms on islands (with respect to that on terraces) which enhances the attempt frequency for atoms to jump over the step edge. The latter is described by the concept of two mobilities [3] and can be obtained for example, by decreasing the island size. This may be realized by the interaction with a surfactant inducing a high nucleation density. The step edge can be influenced directly by the presence of a surfactant inducing structural and electronic changes in the vicinity of a step. Both mechanisms allow us to intensify the interlayer diffusion. For heteroepitaxial film growth, additional complexity is induced. Depending on the lattice mismatch of film and substrate, the film tends to reduce the film and interface energy by structural reconstructions. The latter may strongly influence the surfactant action.

A well studied example is the growth of Cu on clean Ru(0001) in the initial layers [4–8]. The lattice parameter in the Cu(111) surface is 5.5% smaller than that of Ru(0001). This results in a series of different relaxation structures in the first 3–4 ML analysed by STM [5, 6] due to their different corrugation heights and by low energy electron diffraction (LEED) due to the long range order developed [4, 7, 8]. The first Cu layer grows pseudomorphic on the Ru(0001) substrate [4]. The Cu bilayer undergoes a uniaxial reconstruction in order to reduce surface stress in one dimension. It consists of alternating hcp and fcc stacking sequences separated by linear domain walls [5, 6]. The third layer inhibits the same kind of reconstruction in all three close packed [110]-like directions which gives rise to a star structure [5, 6]. Above 3 ML, the Cu film relaxes to a lattice approaching that of Cu(111) which results in a moiré corrugation pattern as investigated by STM [6] and LEED [8]. At temperatures below 450 K also metastable structures develop instead of the moiré, as has been recently investigated by STM [9]. Due to this metastable reconstruction, linear defects develop which tend to arrange in hexagonal and triangular patterns defining domains of the atoms enclosed. They are reproduced on each newly formed Cu layer with a local thickness exceeding 3 ML and the development of a perfectly relaxed Cu(111) film for temperatures below 450 K is retarded [9]. By increasing the growth temperature further or by annealing the film, isolated Cu film plateaus develop which consist of almost relaxed Cu(111) islands located on a base layer of 2 ML–3 ML thickness. Its misfit of 5.5% with respect to the Ru(0001) interface results in a moiré corrugation pattern, as resolved in STM [5, 6] and LEED measurements [8]. By annealing, the film approaches to the thermodynamical equilibrium shape consisting of a closed Cu bilayer and thick Cu(111) islands of relatively small extend. This Stranski–Krastanov morphology is preserved until desorption. In thermal desorption spectroscopy (TDS), three energetically different desorption states can be distinguished, corresponding to multilayer, bilayer and monolayer desorption with rising temperature [7, 10].

By applying an O precoverage on Ru(0001) and subsequent growth of a Cu film, previous Auger electron spectroscopy (AES) [7, 10], ion scattering spectroscopy (ISS) [11] and work function measurements [12] revealed that O is always present on the surface of the grown Cu film. Under certain conditions ($\Theta_O = 0.2$–$0.4$ ML) and temperatures around 400 K, the work function monitored during film evaporation oscillates with a period of 1 ML [12]. This led to the conclusion that O serves as a surfactant for a layer-wise Cu growth on Ru(0001), periodically inducing a high density of islands. The changes in step density during the film growth induces variations in the density of step edge dipoles due to the Smoluchowski effect [13] and is responsible for the change in work function.

Similar results were obtained by investigating Cu/Cu(111) with thermal energy He atom scattering (TEAS) [14]. For $O_2$ preadsorption, the TEAS intensity shows oscillations at 400 K which are interpreted by a periodically changing step length with a high island density.

The aim of the present work is to represent an overview of several STM and LEED investigations which study the growth morphology of Cu films on O-precovered Ru(0001) in detail (see also [15, 16] for more experimental results). To yield a microscopic picture of the surfactant action, $\Theta_O$ is varied systematically. The surfactant structure is characterized by highly resolved STM images. It turns out that misfit-induced defects visible on a Cu film on clean Ru(0001) are also observed for O-surfactant-assisted growth of Cu layers. The temperature dependence of the O-induced Cu film growth (for $\Theta_O = 0.35$ ML and 0.5 ML) led to a discrimination of two different surfactant structures for $\Theta_O < 0.4$ ML and 0.4 ML $< \Theta_O <$ 0.5 ML. We distinguish different mechanisms of 2D layer growth induced by the O/Cu structures and the Cu film defects. These defects together with the locally ordered O/Cu structure induce heterogeneous nucleation [15, 17]. In contrast, the O saturated structure causes homogeneous nucleation and the Cu film defects are not active. Finally, we demonstrate that Cu film growth on a formerly annealed Cu/O/Ru(0001) film system gives a more perfect layer-by-layer growth induced by heterogeneous nucleation at periodically arranged Cu film defect sites. Another study uses the ordered $(3 \times 2\sqrt{3})$ O/Cu layer as a base layer for further Cu film growth. This ordered O/Cu layer is obtained for Cu/O/Ru(0001) film systems at temperatures around 520 K [18] and has been interpreted in terms of the formation of a disrupted $Cu_2O$-like surface oxide layer [16]. A strong correlation of the disordered O/Cu surfactant structure to disordered elements of the $Cu_2O$-like surface oxide layer was revealed by studying further Cu film growth on this structure.

## 2. Experiment

The investigations were performed in an ultrahigh-vacuum chamber with base pressure of $5 \times 10^{-11}$ mbar. The chamber houses an Ar ion gun and a sample heater with electron bombardment for preparation, and a high resolution backview LEED and Auger electron analyser for surface characterization. Rotation of the sample heater allows us to locate the sample in front of a Cu evaporation source or to transfer the sample into the STM operating at room temperature. The details of the experimental setup are described elsewhere [19].

The Ru(0001) crystal with a miscut of less than $0.5^\circ$ was prepared by cycles of Ar ion bombardment followed by heating up to 1300 K. C and S surface contaminations are effectively removed by 20 Langmuir (L) (1 Langmuir $= 1.33 \times 10^{-6}$ mbar s) of $O_2$ adsorption, followed by desorption at 1600 K as described in [7, 20]. The sample heater was initially calibrated by a Ni/NiCr thermocouple, spot welded to the rim of the crystal. Preparation was repeated until LEED shows a clear $(1 \times 1)$ pattern and STM images reveal large clean terraces, about 100 nm in width. Under stable tunnelling conditions, the STM resolves atomic corrugations in the range of 0.01 nm.

O precoverages were performed via a leak valve at a constant pressure of $2 \times 10^{-9}$ mbar at 400 K sample temperature. Our calibration of the O precoverage was done by analysing the LEED spot intensity of the O-induced overlayer on Ru(0001) [21]. At 400 K, $O_2$ adsorbs dissociatively and develops a $p(2 \times 2)$ overlayer saturated for $\Theta_O = 0.25$ ML and a $p(2 \times 1)$ saturated for $\Theta_O = 0.5$ ML. The completion of the $p(2 \times 2)$ gives rise to a sharp intensity maximum of the corresponding LEED spots and is also correlated with a change of slope in the work function rise [22]. The work function linearly correlates with the absolute O coverage. By following the intensity variation of the $p(2 \times 2)$ LEED spots and by determination of the

sharp intensity maximum, we were able to correlate our $O_2$ dose scale to the O coverage on Ru(0001). For details see [21].

The Cu films were prepared by evaporation of Cu with 99.996% cleanliness from a resistively heated W basket. The temperature of the Cu ball inside the basket was controlled by an encapsulated Ni/NiCr thermocouple. A quartz oscillator was used to determine the evaporation rate which was adjusted to about 0.2 ML $min^{-1}$. By heating the crystal to 1600 K, $O_2$ and Cu were completely desorbed and the clean Ru(0001) surface restored.

All STM images are obtained at room temperature after growing the Cu films at different temperatures. Annealing of the Cu films on O/Ru(0001) up to 700 K results in a 2–3 ML thick base layer and ameliorates the ordering of the film defects. We use this layer as substrates to study further Cu film growth at 400 K which is described in the last chapter. In our investigations tunnelling currents of 0.5–2 nA and sample voltages in the range of $-0.05$ V to $-1$ V are used. Under specific tunnelling conditions, the Cu(111) surface and the O-induced surface structures are atomically resolved. Characteristically, we never obtained atomic resolution of the clean metallic surface under tunnelling conditions where the O-induced structures are resolved (typically $-0.5$ V tunnelling voltage and 2 nA current). Only for much lower tunnelling voltages of a few mV could clean Cu be measured with atomic resolution.

## 3. Results

### *3.1. Change of growth by variation of O precoverage*

At the beginning, we present a series of STM images of Cu films on Ru(0001) modified by O preadsorption to give an overview of the film morphologies obtained (figures 1(a)–(c)). The growth temperature was 400 K where in previous work function measurements an O-induced layer-by-layer growth of Cu on Ru(0001) was found.

The growth of Cu films on clean Ru(0001) shows a multilayer morphology, comparable to that obtained for 0.12 ML O precoverage (outside the marked area in figure 1(a)). The surface displays large growth hillocks which are partly covered with isolated areas of small triangularly shaped 2D islands of a high local density (inside the elliptical line). By increasing the O precoverage to 0.2 ML, we obtain a transition to 2D growth (figure 1(b)). Neglecting steps arising from the miscut of the Ru(0001) crystal (see arrows), we observe only three layers exposed simultaneously. On the terraces, monatomic holes and 2D islands are visible. The step edges and the triangular shaped island edges are oriented along [110]-like directions. A high density of 2D islands of about $1 \times 10^{-13}$ $cm^{-2}$ is measured. The islands are inhomogeneously distributed and differ in size. The situation equals that of the locally observed nucleation inside the elliptical line in figure 1(a). The 2D islands are arranged in local clusters which are separated from each other. Each cluster displays different growth stages simultaneously, ranging from nucleation to coalescence.

Applying an O precoverage of $\Theta_O = 0.5$ ML, which corresponds to the saturation coverage on Ru(0001) for O, yields again a different film morphology (figure 1(c)). The film grows still layer by layer, but the islands are of irregular shape and homogeneously distributed. The island density is reduced by a factor of about 10.

As will be shown in detail below, the surface in figures 1(a) and 1(b) is partly covered with an O/Cu surfactant structure where preferential nucleation of Cu atoms is induced. This explains the inhomogeneous island distribution and island size distribution as well. In figure 1(c), the entire surface is covered by an O/Cu surfactant structure which gives rise to an homogeneous distribution of 2D islands. In contrast to a preparation with $\Theta_O = 0.12$ ML and 0.2 ML, no preferential step orientations are found.

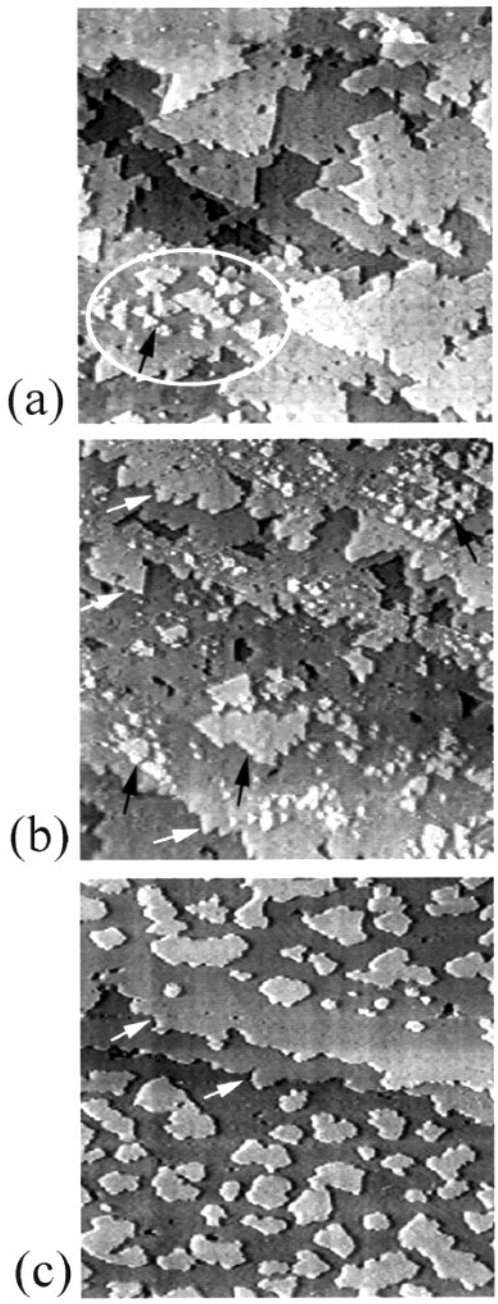


**Figure 1.** STM images of 6.4 ML thick Cu films grown at 400 K with different O precoverages on Ru(0001) resulting in different film morphologies. The images show details of the topography for (a) $\Theta_O = 0.12$ ML, (b) $\Theta_O = 0.2$ ML and (c) $\Theta_O = 0.5$ ML, revealing 3D multilayer growth (a) and layer-by-layer growth with different island shapes and densities (b), (c). The ellipse in (a) and the black arrows in (b) indicate areas of the O/Cu surfactant structure where a locally restricted nucleation takes place. The white arrows in (b), (c) indicate Cu growth in front of steps originating from the miscut of the Ru(0001) substrate. Image size is always 180 nm $\times$ 180 nm.

In the figures 2(a)–2(c), a similar set of experiments in dependence on $\Theta_O$ is presented at higher resolution. The images are obtained for about 6 ML Cu grown at 400 K for different $\Theta_O$. The inhomogeneous appearance of the surface imaged in figure 2(a) for $\Theta_O = 0.12$ ML is most conspicuous. We observe smooth surface areas with a small corrugation height of 0.01 nm corresponding to the clean Cu film surface (denoted by Cu) and isolated areas which are highly corrugated by about 0.06 nm (denoted by O/Cu). A locally restricted nucleation of smooth Cu islands within those surface areas which are highly corrugated is observed. We correlate these highly corrugated areas to the presence of O in the surface layer (compare with figure 2(a)). Their mean surface height is about 0.03 nm higher than the surrounding level of the smooth Cu film and is attributed to a rearrangement of Cu and O atoms. Hence, the expectations from previous AES [7, 10] and work function measurements [12] that O floats into the topmost layers and serves as surfactant for Cu film growth at 400 K are directly confirmed. In the STM images the O/Cu surface structure is in clear contrast to the clean Cu areas which show a low corrugation of less than 0.01 nm. The small triangularly shaped Cu islands (denoted by Cu) are completely surrounded by the O/Cu structure but are not covering the structure. This is concluded from the measured height difference of 0.2 nm from the Cu terrace to the top of the Cu islands (see black line in figure 2(a)) which agrees with the step height of Cu on Cu(111). For $\Theta_O = 0.38$ ML (figure 2(b)), almost the entire surface is covered by the highly corrugated area of the O/Cu structure with the exception of small triangular islands and of island edges (see arrows). The O/Cu structure shows a locally regular hexagonal pattern of protrusions and depressions with a lateral distance of 0.6 nm (see below for details and higher resolved images). This corrugation pattern is interrupted by some linear defect lines of lower height (dark lines, denoted by L). These defect lines are also visible on the clean Cu areas and are independent of the formation of the O/Cu structure (see figure 2(b), left side). The defect lines tend to arrange in closed shapes defining triangular and hexagonal domains of the Cu film. They belong to the formation of metastable Cu film reconstructions [9]. A triangular domain on the Cu film is visible in figure 2(b). We denote it a $\Delta$-defect. In the same image we find triangular Cu islands embedded in the O/Cu structure of the same size and orientation (marked by arrows and denoted by Cu). As will be discussed below in more detail, the $\Delta$-defects, if covered by the O/Cu structure, act as nucleation centres for Cu adatoms, resulting in the formation of triangular islands of the same size. In figure 2(c), we present the morphology of a Cu film for $\Theta_O = 0.45$ ML. Now the entire surface is covered by an O/Cu structure inducing the rough and disordered appearance of the whole surface. The corrugation pattern of protrusions and depressions is less ordered than that for $\Theta_O < 0.4$ ML, although some alignment of protrusions and depressions is visible. It has already been shown that this disordered O/Cu structure drastically reduce the island density and destroys the step edge orientation along [110]-like directions. The depressed linear defects forming triangular and hexagonal shapes are still present, but hardly detectable on the image of figure 2(c). The disordered O/Cu structure bridges these defect lines and behaves like a closed carpet. Additional experiments [15] show that this surface morphology is obtained for all $\Theta_O$ ranging from 0.4 to 0.5 ML.

To gain more insight into the floating process of O on the surface, we have systematically analysed the fractional coverage of the O/Cu structure and the mean island densities ($N$) as a function of $\Theta_O$ as measured by a series of STM experiments. For this analysis we count clean Cu islands and islands covered fractionally by O/Cu together. In figure 3 the results are displayed. The fractional part of the surface covered with the O/Cu structure rises almost linearly with $\Theta_O$ and reaches saturation for $\Theta_O \approx 0.4$ ML. The measured island density $N$ increases by a factor of about 100 from the value of $2 \times 10^{11}$ cm$^{-2}$ for clean Cu and reaches

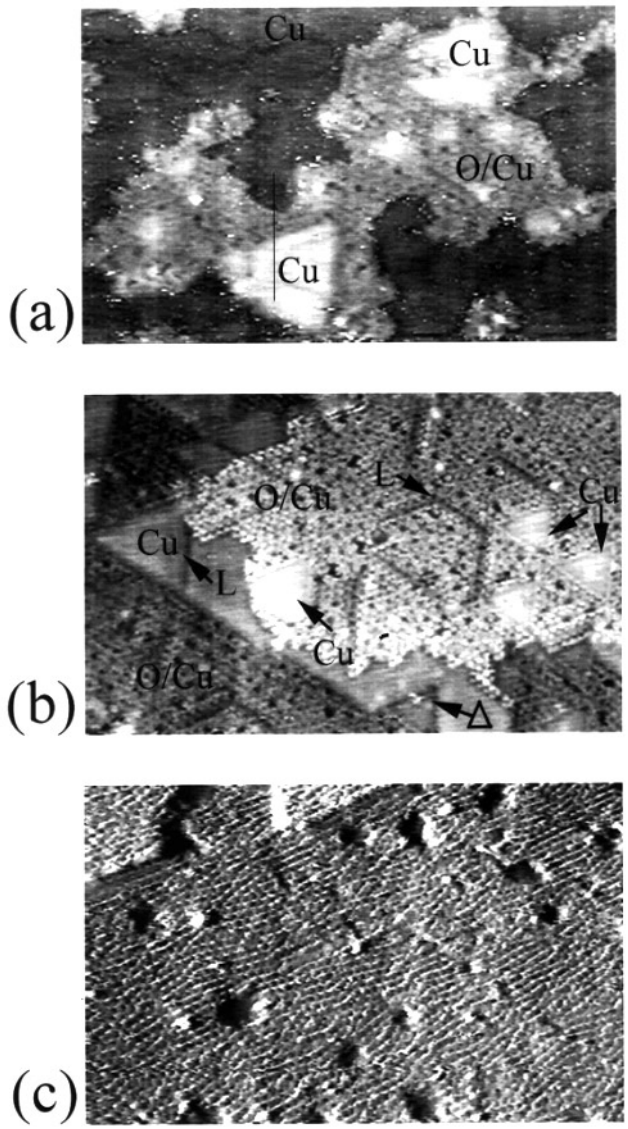


**Figure 2.** High resolution STM images of Cu films grown on O precovered Ru(0001). (a) $\Theta_O =$ 0.2 ML, (b) $\Theta_O = 0.38$ ML and (c) $\Theta_O = 0.45$ ML. (a) and (b) show the locally ordered O/Cu structure established for $\Theta_O$ between 0.1 and 0.4 ML. In (a) and (b) is a clear difference in corrugation between the smooth Cu film areas (indicated by Cu) and the highly corrugated O/Cu islands (indicated by O/Cu). Note the smooth, triangular Cu islands in (b) which are surrounded by the O/Cu corrugation (marked by arrows). $\Delta$ denotes a triangular defect in the Cu film. The $\Delta$-defect is of the same size and orientation as the Cu islands. L denotes defect lines, visible on clean Cu and on the O/Cu structure. (c) displays the saturated O/Cu structure established for $\Theta_O$ between 0.4 and 0.5 ML. All films have a nominal thickness of about 6.4 ML and were grown at 400 K. Image size is always 40 nm $\times$ 33 nm.

its maximum value also for $\Theta_O \approx 0.4$ ML. By increasing $\Theta_O$ further, a sudden drop in the island density occurs by a factor of 10 and no further changes occur up to $\Theta_O = 0.5$ ML. This transition is accompanied by the structural change of the locally ordered O/Cu structure to a

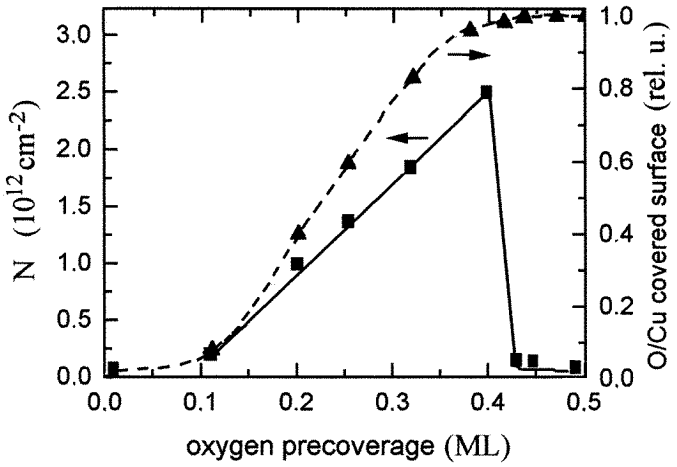


**Figure 3.** Nucleation density (full line, corresponding to the left axis) and fractional surface coverage (dashed line, corresponding to the right axis) of the O/Cu surfactant layer which is deduced from STM images for O-modified Cu film growth on Ru(0001) at 400 K as a function of $\Theta_O$. An abrupt reduction of the nucleation density occurs for $\Theta_O > 0.4$ ML. It is accompanied by a structural change of the O/Cu surfactant layer. For details see text.

disordered arrangement and a loss of the preferential step edge orientation. Both structures are of short range order; only the $(1 \times 1)$ LEED pattern of Cu(111) was obtained.

The diagram demonstrates that the onset of the floating process of O on the surface is retarded and starts for about $\Theta_O \approx 0.1$ ML. This corresponds to previous AES [7, 10] and ISS [11] studies which suggest that a fraction of the O remains at the Cu/Ru(0001) interface. However, recent investigations by x-ray photoelectron diffraction [23] imply that the O-interface is free of O. Up to now the observed retarded float out of O is not yet clarified. Probably the O is partly trapped by the misfit induced defects within the bulk Cu.

At $\Theta_O = 0.4$ ML, the surface is completely covered by the locally ordered O/Cu structure. Because of this saturation value, we assume the ratio of O:Cu on the surface to be about 1:2. This agrees with the number of depressed sites obtained from a highly resolved STM image of the locally ordered O/Cu structure (see below). One might assume that the disordered O/Cu structure (which appears for 0.4 ML $< \Theta_O <$ 0.5 ML) has a certain higher density of O atoms and this excess O destroys the hexagonal ordering. The disordered O/Cu structure corresponds therefore to an over-saturated O/Cu phase.

Both O/Cu structures (for 0.1 ML $< \Theta_O <$ 0.4 ML, denoted in [15] as the ordered or the A-type structure and for 0.4 M $< \Theta_O <$ 0.5 ML, denoted as the disordered or the B-type structure) act as surfactants for Cu film growth but strongly differ in the resultant film morphology and island density. The corresponding mechanism of surfactant action are expected to be different and will be described below in more detail.

### *3.2. Surfactant mechanisms induced by the ordered O/Cu structure*

The Cu islands within the ordered O/Cu structure are always of triangular shape. In the nucleation stage, we always observe small triangular islands of a uniform size (see figure 2(b)). In [17] we have shown that a high degree of heterogeneous nucleation of these small triangular islands could be achieved by Cu evaporation on a formerly annealed Cu film on O-precovered

Ru(0001). We have demonstrated that the annealing induces a high density of triangular Cu film defects (denoted as $\Delta$-defects) which are periodically arranged in a quasihexagonal superlattice [9]. If covered with the ordered O/Cu surfactant structure, the $\Delta$-defects induce heterogeneous nucleation of Cu adatoms [24]. The result of such an experiment is shown in figure 4(a). A 3 ML thick Cu film on O/Ru(0001) with $\Theta_O = 0.4$ ML was annealed to 600 K and covered with 7.2 ML Cu at 400 K. The image displays a surface partly covered with the ordered O/Cu surfactant structure. The mobility of Cu adatoms on these areas is rather low. The latter are decorated by small and periodically arranged triangular Cu islands of the same size and shape as the initial $\Delta$-defects. In contrast the mobility of Cu adatoms on clean Cu areas and islands is high because of the low surface diffusion barrier of $E_d = 0.05$ eV as deduced for Cu adatoms on Cu(111) [25, 26]. Cu nucleation and growth is therefore restricted to that surface parts covered with the ordered O/Cu structure. The deposited Cu atoms are captured within the triangular $\Delta$-defects (as visible in figure 2(b)), whose boundaries reflect the diffusion Cu adatoms [24]. The small triangular Cu islands which develop just after nucleation of Cu adatoms act as traps for a further 2D Cu film growth.

The linear Cu film defects, the hexagonal arranged defect lines and the $\Delta$-defects (see figure 2(b)) are already observed on the clean Cu film on Ru(0001). This is demonstrated by figure 4(b). A Cu film of 5 ML thickness was grown at 400 K on Ru(0001). We attribute the hexagonal defect pattern to an incompletely relaxed Cu film and have shown that it results from metastable relaxation structures originating in the third Cu layer [9]. This hexagonal pattern is resolved in nearly atomic resolution together with a triangular shaped Cu film defect in figure 4(b). A hexagonal domain consists of Cu atoms with continuously changing adsorption sites ranging from hollow to almost on-top positions and has a threefold symmetry. An atomic model of this 'hexagon' is presented in [9]. The $\Delta$-defects emerging on the incompletely relaxed Cu film together with the ordered O/Cu structure covering these defects are responsible for the heterogeneous nucleation and the high island density of $2 \times 10^{-12}$ cm$^{-2}$ observed for $0.1$ ML $< \Theta_O < 0.4$ ML [15]. An atomic model of the $\Delta$-defects is presented in figure 4(c) and is described in more detail in [9]. In this context, the $\Delta$-defects can be explained by a locally induced reconstruction of Cu atoms which otherwise would occupy on-top sites of a non-rotated moiré pattern of the Cu(111) film.

In contrast, the smooth areas of a thick Cu film (more than 10 ML) grown at higher temperatures show the moiré-like corrugation pattern of the perfectly relaxed and slightly rotated Cu(111) film on Ru(0001) and the $\Delta$-defects are not observed [5, 6]. Even in the presence of an ordered O/Cu structure (on a Cu film that shows the moiré pattern) prepared by O preadsorption [16, 27] and postadsorption [16] at 520 K, triangular islands were not observed.

In the following we present a scenario of growth of Cu films on the ordered O/Cu structure deduced from the STM images of figures 1(a), 1(b) and 2(a), 2(b). In figures 1(a), 1(b), 2(a), different isolated growth centres are visible (see arrows) where larger islands are surrounded by smaller ones. We therefore assume a lateral displacement of the O/Cu structure induced by growing Cu islands embedded in this structure. Small Cu islands (representing a growth stage just after nucleation) consist always of clean Cu whereas large islands (representing an older stage of growth) are partly covered with the surfactant structure. Cu adatoms impinging on small O-free Cu islands are rather mobile and can therefore overcome the step edge barrier, because of a high attempt rate. In contrast, the Cu adatoms on the O/Cu structure are quickly captured by the $\Delta$-defects of the Cu film or at step sites. This situation corresponds to the concept of two mobilities [3] where the 2D growth can be explained by an increase of the attempt rate of Cu adatoms for step descent. The growing Cu islands laterally displace the surfactant structure into peripheral directions out of the local growth centres and induce further nucleation

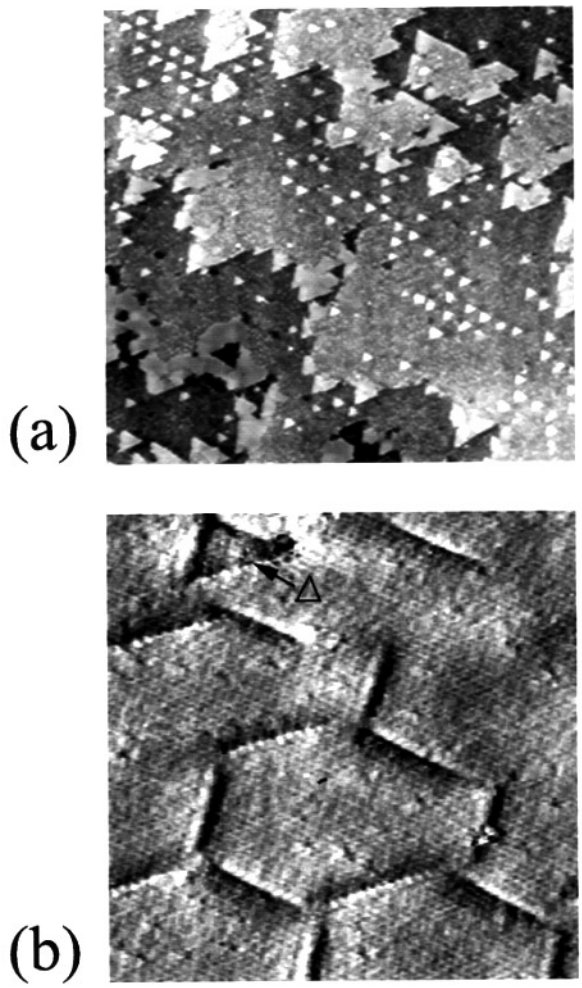


**Figure 4.** Heterogeneous nucleation induced by the locally ordered O/Cu structure at the Δ-defects of the Cu film (a). After growing a 3 ML thick Cu film at 400 K (with $\Theta_O = 0.4$ ML) the sample was annealed up to 600 K. Finally about 7.2 ML Cu were postdeposited at 400 K. For explanations see text. Image size is 120 nm × 120 nm. (b) displays Cu film defect structures on a 6 ML thick Cu film on Ru(0001) grown at 400 K. The hexagon structure is nearly atomically resolved and a Δ-defect (denoted by Δ) is visible. Image size is 13 nm × 13 nm. (c) displays an atomic model of the Δ-defects. The model is based on an incompletely relaxed Cu(111) film (0.258 nm lattice parameter) located on the Ru(0001) (0.276 nm lattice parameter) resulting in a moiré corrugation pattern. It is assumed to be non-rotated (in contrast to the rotated moiré observed at higher temperatures [6, 8]). Atoms of the energetically unfavourable on-top positions of the moiré are removed and replaced in such a manner that most of them occupy fcc hollow sites forming triangular domains. The model size is 11 nm × 11 nm. For more details see [9].

on formerly clean Cu areas. Larger islands are therefore surrounded by smaller ones. The areas of the small islands represent a spreading front of nucleation, where the nucleation actually takes place. The lateral displacement of the O surfactant continues until different surfactant areas contact each other. During coalescence of the Cu islands the surfactant structure is forced to spill on top of the islands and the growth process repeats itself maintaining a 2D

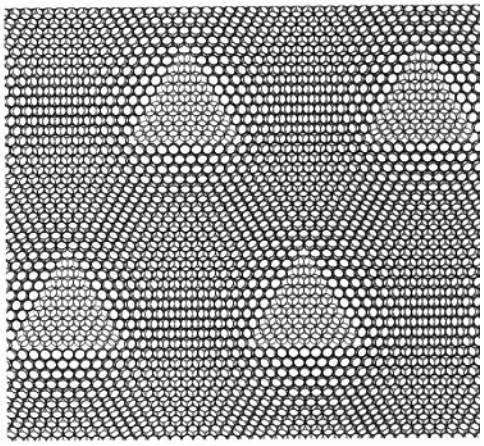


**Figure 4.** (Continued)

growth. However, the detailed mechanism of O segregation on top of the surface is still an open question. We assume that bonded O–Cu–O strings migrate on the surface (see discussion below and in [16]). The lateral displacement of the surfactant on formerly clean Cu areas explains the wide range of precoverages of 0.2–0.4 ML (and also in the corresponding O surface coverage) where a 2D growth is observed. For $\Theta_O = 0.12$ ML, the nucleation is restricted within isolated O/Cu areas, inducing mutlilayer growth as observed in figure 1(a). Here, the coalescence of small Cu islands proceeds faster than that of the lateral expanding O/Cu surfactant areas. This results in a locally restricted nucleation, causing the formation of 3D hillocks. By slightly increasing $\Theta_O$ to 0.2 ML, sufficiently large surfactant islands exits, each representing a localized growth centre, which are able to contact and therefore induce 2D growth. By increasing $\Theta_O$ to 0.4 ML, the whole surface is covered by the surfactant with the exception of small Cu islands. In contrast to the localized growth centres (for $\Theta_O = 0.12$ ML and 0.2 ML) which exhibit different growth stages, an almost homogeneous growth stage is present at a certain time. This makes sure that nucleation of a new layer starts after coalescence of the last one.

We now consider the difference of the surfactant action between the ordered and disordered O/Cu surfactant structure. For this, we investigate the temperature dependence of Cu films grown on O-precovered Ru(0001) for $\Theta_O = 0.35$ ML and $\Theta_O = 0.50$ ML. These coverages represent the influence of the ordered and disordered surfactant structure. We have performed STM investigations of Cu films of about 6 ML thickness on O/Ru(0001) at different temperatures ranging from 300 K to 450 K. In [15] we have presented images of the growth morphology for Cu films prepared with $\Theta_O = 0.35$ ML at 330 K and 380 K. The growth mode changes drastically from 3D hillock growth (300 K) to a layer-by-layer growth at 380 K (see [15]). STM images obtained with higher resolution reveal that the same surfactant structure is present on the surfaces of the Cu films grown at 330 K and 360 K (not shown). An analysis of the island densities gives a value of about $1 \times 10^{12}$ cm$^{-2}$ almost independent of temperature from 300 K to 420 K, as can be seen from a plot in an Arrhenius diagram (figure 5, dashed line). We take this behaviour as an additional indication for the previously discussed heterogeneous nucleation on the locally ordered O/Cu structure.

Similar experiments were performed for Cu films grown at temperatures ranging from 300 K to 450 K with $\Theta_O = 0.5$ ML (see [15]). As a function of temperature the same

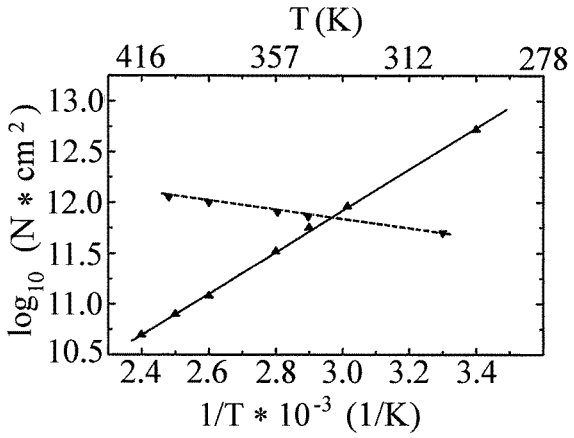


**Figure 5.** Temperature dependence of Cu film growth on O/Ru(0001) in terms of an Arrhenius plot. The island density $N$ as derived from a series of STM measurements, where Cu films of about 6 ML thickness were deposited at different temperatures (300 K–450 K). The analysis was performed for two different O precoverages of 0.32 ML (▼) and 0.5 ML (▲).

growth regimes were obtained. The disordered O/Cu structure was always present on the surface. In contrast to the island densities for $\Theta_O = 0.35$ ML which are nearly independent of temperature, we observe a steep continuous decrease of island densities with temperature (from $5 \times 10^{12}$ cm$^{-2}$ at 300 K to $3 \times 10^{10}$ cm$^{-2}$ at 420 K). By plotting the temperature dependency of the island density in an Arrhenius diagram (full line in figure 5), a nearly perfect linear behaviour was obtained. This is a signature of homogeneous nucleation. We assume that the disordered O/Cu structure covers the Cu film like a closed carpet which deactivates the $\Delta$-defects as nucleation sites. The Cu adatoms migrate on top of the disordered O/Cu structure and are influenced by its specific diffusion barriers. Occasionally, they penetrate the surfactant layer in order to form nuclei or being incorporated at steps. From the slope of the Arrhenius curve we have determined a surface diffusion energy barrier of $E_d = 0.9$ eV which is a rather high value compared to that of the clean Cu film of about 0.03–0.05 eV [25, 26]. The Cu adatom diffusion on the disordered O/Cu structure is therefore strongly restricted which explains the enhanced nucleation density at 400 K. Because all growing Cu islands are immediately covered by the O/Cu structure, the concept of two mobilities is not applicable to understand the 2D growth. Instead, we found a reduction of the interlayer diffusion barrier from $E_s = 0.16$ eV for clean Cu films to a value of 0.08 eV by an analysis of the Cu islands formation on the saturated O/Cu structure [15]. The latter effect drastically enhances interlayer diffusion which immediately explains the observed layer-by-layer growth.

The work function oscillations reported previously [12] indicate a narrow temperature interval ranging from 350 to 420 K where layer-periodic oscillations exist. One has to take into account that measurable work function changes presuppose a large variation in step density. Therefore a layer growth with a small variation of island density results only in minor changes of total step length during the growth period of one layer and does not induce measurable work function changes. The STM investigations yield the maximum density of islands for the ordered O/Cu surfactant structure. Obviously, the work function oscillations monitor the 2D island growth on the ordered O/Cu surfactant structure with its large variation in total step length. In contrast, the film growth on the disordered surfactant structure did not result in measurable work function changes.

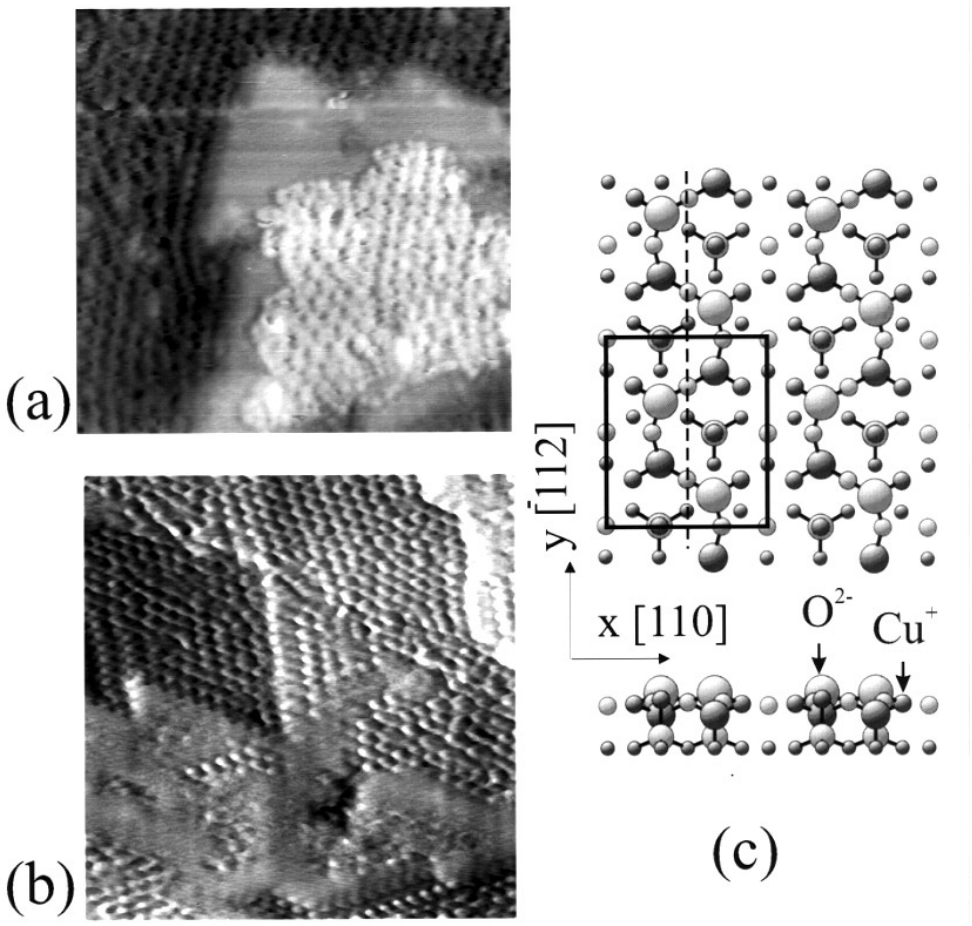


**Figure 6.** High resolution STM images of 5 ML thick Cu films on Ru(0001) grown at 400 K, (a) with $\Theta_O = 0.35$ ML precovered, (b) after postadsorption of 40 L $O_2$ on the clean Cu film. The smooth areas display clean Cu, whereas the zigzag-like corrugation pattern is induced by the O/Cu structure. Image size is always 15 nm × 15 nm. (c) presents an atomic model of the disrupted $Cu_2O$ sandwich-like structure composed of (111) planes of Cu and O, as deduced from LEED investigations. The upper part presents the on top view and the lower part a cross section of the O/Cu/O/O/Cu five plane system. The unit cell of the $(3 \times 2\sqrt{3})$ lattice is indicated. The axis of glide plane symmetry is denoted by the dashed line.

### *3.3. Structures of the O/Cu surfactant layers*

To obtain more insight into the locally ordered surfactant structure, we display it in a high resolution image in figure 6(a). The film consists of 5 ML Cu grown on O-precovered Ru(0001) at 400 K with $\Theta_O = 0.35$ ML. To induce a higher degree of ordering the film was slightly annealed to 480 K and thereafter covered by 1 ML Cu at 400 K. This preparation results in a locally well ordered surfactant structure. Parallel aligned zigzag-like rows of depressions are clearly visible.

The O/Cu structure in figure 6(a) indicates that the protrusions or depressions are arranged in a distorted hexagonal lattice. The assignment of either the depressions or the protrusions measured by STM to the O sites is problematic. In the literature O atoms were usually assigned

to depressions for O/Cu(110) and O/Cu(100) [28]. In contrast for O/Cu(111), the depressions were interpreted as holes in the O/Cu structure [29]. Assuming the depressions to be O atoms according to [28], we derive a density of O atoms within the ordered O/Cu structure of 0.33 by counting all of the visible depressions arranged in zigzag-like rows (small dots in figure 6(a)). For $\Theta_O = 0.4$ ML, the surfactant covers the surface entirely, which corresponds to a surface coverage of O atoms of about 0.33 ML. In figure 6(b), we display a surface of a 6 ML thick Cu film grown on Ru(0001) at 400 K which is exposed subsequently to 40 L $O_2$ at 400 K. In addition to the smooth Cu islands we observe a similar corrugation pattern as resolved on the ordered O/Cu structure. Lines of zigzag rows are visible. Neighbouring zigzag rows are separated and shifted against each other, defining a hexagonal pattern of depressions. Step edges of the Cu film appear with a saw-tooth-like corrugation induced by adsorption of O atoms at steps (see lower part of figure 6(b)). The zigzag lines with their small depressions and protrusions most probably consist of O–Cu–O strings. The corrugation height level of the depressions is lower than the medium level of the Cu film, whereas the protrusions exceed it. We explain this by a strong binding of Cu and O atoms which modifies the electron density near the Cu atoms in comparison to that of the metallic film.

We conclude that $O_2$ postadsorption on Cu films at 400 K induces restructuring of the Cu film similar to that obtained by the locally ordered O/Cu surfactant structure for $\Theta_O < 0.4$ ML. By increasing the $O_2$ dose to more than 200 L in postadsorption experiments (not shown), the entire surface is covered by the O/Cu structure which grows laterally.

In a previous paper [16] we have investigated ordered O/Cu structures obtained by pre- and postadsorption of $O_2$ on Cu/Ru(0001) at elevated temperatures with different film thickness. For $O_2$ preadsorption, the O/Cu structure consists of a periodic, disrupted hexagonal lattice which develops in the first and second Cu layer and gives rise to a LEED pattern [8, 18]. A $(3 \times 2\sqrt{3})$ periodicity with a glide plane symmetry was obtained. The derivation of an atomic model for this structure is not unique from a LEED pattern analysis. However, the constraint of a glide plane symmetry and an estimated O content of 0.3 ML–0.5 ML is immediately fulfilled by a disrupted '$Cu_2O$'(111) structure where a Cu layer is sandwiched between two O layers. The $(3 \times 2\sqrt{3})$ periodicity can then be explained by a simple disruption of the p$(2 \times 2)$-O sublattices in the ideal $Cu_2O(111)$ structure parallel to a [112]-like direction [16]. Each O layer contains an amount of 1/6 ML, hence the content of 0.33 ML or 0.5 ML is distributed over two or three O layers, respectively. On the basis of those data a model of a '$Cu_2O$'-like structure was developed and is presented in figure 6(c). Most obvious is the zigzag-like arrangement of O–Cu–O links along the [112] direction where the O atoms are located in different layers. A hexagonal distorted lattice is visible in the model (as well as in figure 6(a), by connecting the small protrusions of neighbouring zigzag rows) by combining the rows of neighbouring zigzag O–Cu–O chains in the perpendicular direction. In our STM images (see also [16]), however, we found that the measured corrugations and symmetry of the atomic arrangement strongly depend on tunnelling conditions. Therefore an exact correspondence of the measured atomic positions with that in the model was not derived. However, the measured corrugations of the O/Cu structure also show elements of zigzag lines and a distorted hexagonal pattern of the same size as proposed by the model. The observed structure is similar to that found for O/Cu(111) [29]. There the authors also propose hexagonal elements of $Cu_2O$ in the (111) plane which are locally incommensurate to explain the observed corrugation pattern.

Postadsorption of 200 L $O_2$ at 520 K on Cu/Ru(0001) films exceeding 3 ML yields only O/Cu structures of short range order. By further increasing the dose up to 1000 L no changes in the structure occur as indicated by LEED and STM investigations [16]. The O/Cu structures found on these Cu films at 520 K consist of similar hexagonally arranged O–Cu–O chains as locally observed in figures 6(a) and 6(b).

The disordered structure of the O/Cu surfactant layer obtained for $\Theta_O = 0.4$–$0.5$ ML is not observed in $O_2$ postadsorption experiments and can be ascribed to an over-saturated O/Cu layer. The surface coverage of O atoms in the saturated structure must exceed 0.33 ML which results in a less ordered structure. The O-induced reconstruction lost the geometrical ordering and the threefold symmetry of the Cu(111) film.

For the disordered O/Cu surfactant layer, we assume also a strong correlation to the $(3 \times 2\sqrt{3})$ O/Cu structure. In particular, we assume that it is also composed of O–Cu–O links which form bent O–Cu–O strings arranged in a more random-like manner [24]. The corresponding investigations are described in the following section.

### *3.4. Cu growth on Cu/O/Ru(0001) substrates prepared at higher temperatures*

Besides the already investigated growth of Cu films on O precovered Ru(0001) we used Cu/O/Ru(0001) film systems prepared at higher temperatures (520 K–700 K) as a substrate to study further Cu growth at 400 K. These experiments were carried out to introduce a higher degree of order in the morphology of the Cu films and the O/Cu surfactant layer, respectively. The Cu/O/Ru(0001) film systems were prepared in two different ways. In the first part we present results of Cu growth on a formerly annealed up to 700 K Cu/O/Ru(0001) film system with $\Theta_O = 0.35$ ML. In the other part, Cu growth was studied on a Cu/O/Ru(0001) system, obtained by depositing 5–10 ML Cu on O-precovered Ru(0001) at 520 K with $\Theta_O = 0.5$ ML.

Intermediate short annealing of Cu films on O/Ru(0001) (with $\Theta_O = 0.35$ ML) up to 800 K results in an enhancement of the work function oscillation amplitude during further Cu growth at 400 K, as already reported [12]. AES and LEED analysis of annealed films indicate the formation of two or three Cu base layers covered with an O/Cu structure during film annealing; the excess Cu is bound in 3D hillocks. These conclusions are directly confirmed by our STM investigations. STM images display large flat terraces of Cu layers covered with the ordered O/Cu structure (see [17]). The corrugation of the O/Cu surfactant structure is modulated by the reconstruction pattern of the second and third Cu layer, indicating a 2 and 3 ML thick Cu film as a base layer. This is confirmed by LEED analysis which shows the characteristic diffraction patterns of the reconstructions of Cu bi- and trilayers of Cu/Ru(0001) [8]. In figure 7, we present STM images of further Cu film growth at 400 K on such a formerly annealed Cu film (with $\Theta_O = 0.35$ ML). After annealing, a 3 ML thick Cu base layer was obtained which displayed smooth and large terraces (typical extension about 100 nm). The series of images with 0.2 ML Cu deposition (figure 7(a)), 0.45 ML Cu (figure 7(b)), 0.75 ML Cu (figure 7(c)) and 0.95 ML (figure 7(d)) reveals different growth stages of a nearly perfect layer-by-layer growth. The surface is almost completely covered by the ordered O/Cu surfactant layer. Cu film growth on the annealed Cu/O/Ru(0001) system starts by formation of small triangular Cu islands which are almost homogeneously distributed on the terraces. In the vicinity of steps, the Cu island density is reduced, caused by capture of Cu adatoms at step sites (figure 7(a)). Further Cu deposition of 0.25 ML results in growth of the trigonal Cu islands which are almost uniform in size (figure 7(b)). In figure 7(c) with 0.75 ML Cu deposition, these islands have already coalesced leaving triangular shaped holes of monatomic depth. Even at this stage all Cu adatoms impinging on the islands cross the step edges and fill the holes. Nucleation of the next layer was first observed for 0.95 ML Cu deposition (figure 7(d), upper right side). On the terraces the adatoms fill the monatomic holes still left. This almost perfect layer growth is repeated for several Cu layers deposited as investigated by STM (not shown). In figure 8 we display an analysis of the initial layer growth on the annealed film in terms of a diagram, where the fractional surface coverage of the exposed Cu layers as a function of deposited Cu is

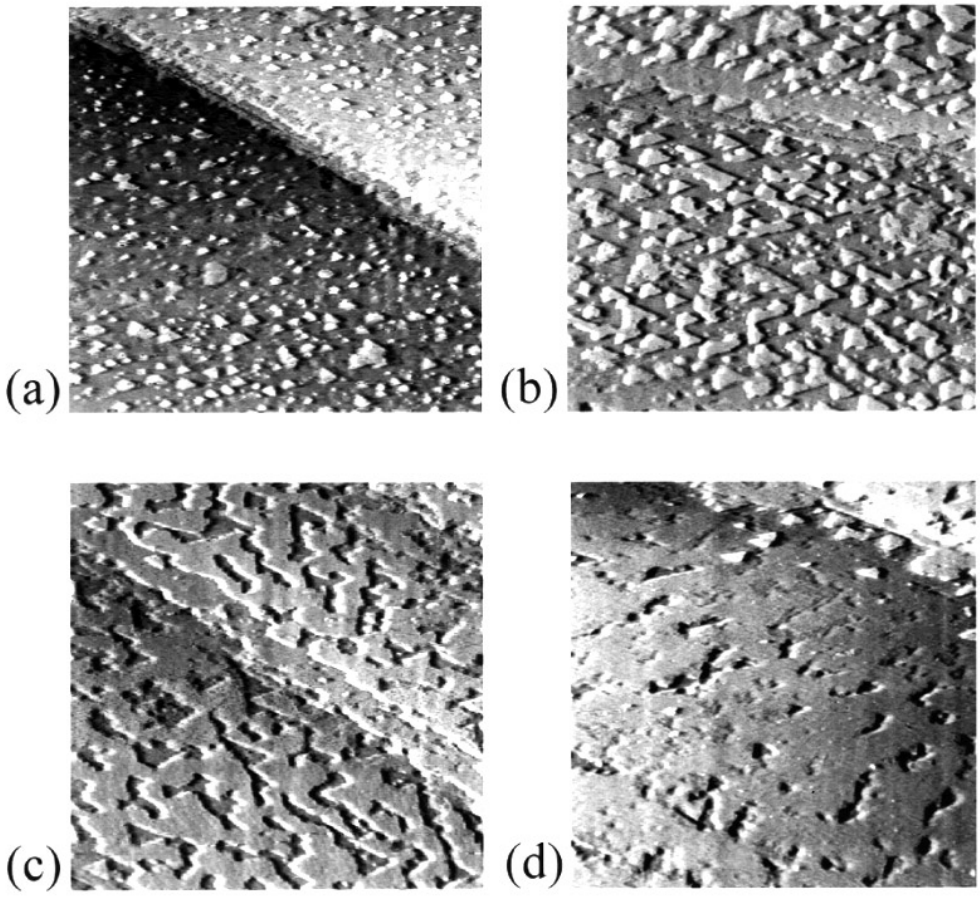


**Figure 7.** Cu film growth on a formerly annealed to 700 K 5 ML thick Cu film on O/Ru(0001) with $\Theta_O = 0.35$ ML. The local film thickness after annealing amounts to 3 ML. The series (a)–(d) demonstrates a perfect layer-by-layer growth for subsequent depositions of Cu at 400 K: (a) for 0.2 ML Cu, (b) for 0.45 ML Cu, (c) for 0.75 ML Cu and (d) for 0.95 ML Cu deposited. In each image three terraces (one of them is rather narrow) are visible. Image size is always 180 nm $\times$ 180 nm.

drawn. Its linear slope and monolayer separation of the curves demonstrates the high quality of layer growth.

The 2D growth starts on top of the 3 ML thick Cu base layer obtained by annealing of the Cu/O/Ru(0001) film system. As already discussed, the reconstructions of this Cu layer are responsible for the formation of triangular Cu film defects which in conjunction with the ordered O/Cu surfactant structure act as nucleation centres for Cu adatoms, inducing heterogeneous nucleation [15, 24] with a high density of periodically arranged $\Delta$-defects. This results in an almost uniform distribution of growing Cu islands (see figure 7(b)) with a maximized island density of about $1 \times 10^{13}$ cm$^{-2}$. In figure 7(a) the small islands are almost free of O whereas in figure 7(b) the larger islands are already covered with the O/Cu surfactant structure. In each growth stage we observe a narrow and uniform size distribution of the growing islands. This results in a defined length (given by the mean island separation) for Cu adatom diffusion until they are captured at step sites. Obviously the mean free path length of Cu adatoms always exceeds this length; the latter corresponds to the separation of defect sites of the Cu film.

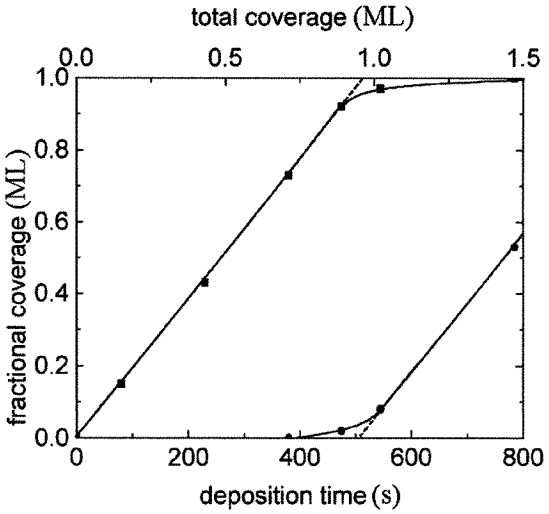


**Figure 8.** Analysis of the film growth as displayed in figure 7 in terms of a diagram where the fractional coverage of the first two growing layers is displayed as a function of the total coverage and deposition time, respectively. It indicates a nearly perfect layer-by-layer growth for the additional deposition of 1.5 ML Cu on a formerly annealed Cu/O/Ru(0001) film system of 5 ML thickness.

The Cu film defects are reproduced in each newly formed layer and the Cu film is kinetically hindered to completely relieve film stress (see [9, 24]).

We now turn to Cu films which were prepared by deposition of 5–10 ML Cu at 520 K on O-precovered Ru(0001) with $\Theta_O = 0.5$ ML and used as substrates for further Cu film growth at 400 K [27]. The films display a transition to Stranski–Krastanov growth with large and smooth 3D islands (size about 300 nm). The local island height only slightly exceeds the mean film thickness. On top of the islands, the $(3 \times 2\sqrt{3})$ O/Cu structure is present (see model in figure 6(c)) as was revealed by LEED [16]. Additional Cu deposition at 400 K again yields a layer-by-layer growth resulting in the same island density and film morphology as observed for the disordered O/Cu surfactant layer. Initially, on top of the Cu islands domains of the $(3 \times 2\sqrt{3})$ O/Cu structure are present. However, the size of these domains drastically decreases with film thickness. After deposition of a few additional Cu layers the periodic ordering was completely destroyed and the O/Cu surface structure appears similar to that of the disordered O/Cu surfactant structure. This similarity led to the conclusion that the structural compositions of both O/Cu structures are comparable on a local scale. As discussed above, a sandwich-like model of a disrupted '$Cu_2O$' surface structure is able to explain the $(3 \times 2\sqrt{3})$ structure (see figure 6(c)). On the surface O–Cu–O chains form zigzag lines and correspond to a sandwich-like layer system where $O^{2-}$ anions enclose $Cu^{+}$ cations. We assume that during the Cu film growth at 400 K this structure is gradually disturbed. Only O–Cu–O strings may survive which arrange in a stochastic manner. Correspondingly, we assume that the disordered O/Cu surfactant structure is also composed of stochastically arranged O–Cu–O strings.

The $Cu_2O$-like $(3 \times 2\sqrt{3})$ structure is formed already in the first Cu layer on Ru(0001). This is directly confirmed by STM which reveals a restructuring of 1–2 ML thick Cu films induced by adsorbing O at 520 K. The $(3 \times 2\sqrt{3})$ ordering is accompanied by an erosion of the first and second Cu layer [8]. However, by $O_2$ postadsorption on Cu trilayers and thicker films where the strain is considerably reduced, no $(3 \times 2\sqrt{3})$ ordering could be induced. We

conclude that the strain of the first Cu layers promotes the formation of the $(3 \times 2\sqrt{3})$ structure, i.e. these layers may act like a catalyst. Once this structure is formed, elements of it float on top of the growing film and act as a surfactant layer for further Cu film growth.

## 4. Summary

The growth of Cu on O-precovered Ru(0001) was investigated by means of STM and LEED. Our results reveal that O serves as a surfactant for layer-by-layer growth of Cu films on Ru(0001) around 400 K. By variation of O precoverage different O/Cu surface structures and 2D island morphologies are obtained. The surface covered by the O/Cu structure rises linearly with precoverage and covers the whole surface for $\Theta_O = 0.4$ ML. For lower $\Theta_O$, a high density of triangular islands partially covered with an O/Cu surfactant structure was found. The O/Cu structure is locally ordered in a distorted hexagonal lattice. Its O density is estimated to be 0.3 ML as deduced from STM images and previous AES results. The structure is assumed to consist of O–Cu–O strings inducing the observed corrugation. The locally ordered hexagonal pattern was interpreted in terms of fragments of a surface oxide of $Cu_2O$. A study of Cu growth on a formerly annealed O/Cu structure on Ru(0001) reveals that the uniform island shape and its high density are caused by heterogeneous nucleation. The latter originates in triangular Cu film defects, which, if covered by the O/Cu structure, act as traps for the nucleation of Cu adatoms. By lateral displacement of the rather mobile O/Cu structure nucleation of Cu adatoms and island growth was induced on formerly clean Cu areas, because adatom mobility is drastically reduced on the O/Cu structure compared to that on clean Cu. The 2D film growth is explained by the concept of two mobilities. For an O content lower than 0.15 ML a 3D growth with locally restricted nucleation on O/Cu areas occurs.

A drastic change of the 2D surface morphology and the O induced surface structure occurs for $\Theta_O > 0.4$ ML up to the saturation value of 0.5 ML. The island shapes are found to be irregular and its density is strongly reduced. From a study of the temperature dependence of island densities an Arrhenius-like behaviour is deduced and a high barrier for surface diffusion ($E_d = 0.9$ eV) obtained. The 2D growth proceeds by homogeneous nucleation on a rather disordered O/Cu surfactant structure. The Cu film defects are inactive as nucleation centres and completely covered by the carpet-like disordered O/Cu structure. The 2D film growth is explained by a reduction of the additional step edge barrier. The O content of the disordered O/Cu layer was estimated to be 0.5 ML and is interpreted to be composed of disordered O–Cu–O strings related to the incomplete formation of a $Cu_2O$-like surface oxide. A well ordered $(3 \times 2\sqrt{3})$ O/Cu structure was obtained by preparing Cu/O/Ru(0001) film systems at higher temperatures or by $O_2$ postadsorption. It was interpreted in terms of a disrupted $Cu_2O$-like oxidized surface closely related to the local structure of the O/Cu surfactant layers.

Previous x-ray photoelectron spectroscopy (XPS) studies performed by annealing Cu films on Ru(0001) in $O_2$ atmosphere indicate the formation of a bulk Cu oxide [18] which has been identified as $Cu_2O$. Future investigations should clarify the expected correlation of the disordered surfactant structure and the formation of a bulk-like $Cu_2O$ on Ru(0001).

## Acknowledgments

HW gratefully acknowledges the support by the Deutsche Forschungsgemeinschaft through the Graduiertenkolleg ‘Defektstruktur-bestimmte physikalische Eigenschaften’. KM and ChA thank the Kultusministerium des Landes Sachsen-Anhalt for support.

## References


[1] Schwoebel R L and Shipsey E J 1966 *J. Appl. Phys.* **37** 3682
[2] Ehrlich G and Hudda F G 1966 *J. Chem. Phys.* **44** 1039
[3] Rosenfold G, Poelsema B and Comsa G 1995 *J. Cryst. Growth* **151** 230
[4] Park C, Bauer E and Poppa H 1987 *Surf. Sci.* **187** 86
[5] Poetschke G, Schröder J, Günther C, Hwang R Q and Behm R J 1991 *Surf. Sci.* **251/252** 592
[6] Günther C, Vrijmoeth J, Hwang R Q and Behm R J 1995 *Phys. Rev. Lett.* **74** 754
[7] Kalki K 1992 *PhD Thesis* Universität Bonn
[8] Ammer Ch, Meinel K, Wolter H, Beckmann A and Neddermeyer H 1997 *Surf. Sci.* **375** 302
[9] Meinel K, Wolter H, Ammer Ch and Neddermeyer H 1998 *Surf. Sci.* **401** 434
[10] Kalki K, Schick M, Ceballos G and Wandelt K 1993 *Thin Solid Films* **228** 36
[11] Shen Y G, O'Connor D J, van Zee H, Wandelt K and MacDonald R J 1995 *Thin Solid Films* **263** 72
[12] Wolter H, Schmidt M and Wandelt K 1993 *Surf. Sci.* **298** 173
[13] Smoluchowski R 1941 *Phys. Rev.* **60** 661
[14] Wulfhekel W, Lipkin N N, Kliewer J, Rosenfeld G, Jorritsma L C, Poelsema B and Comsa G 1996 *Surf. Sci.* **348** 227
[15] Wolter H, Meinel K, Ammer Ch and Neddermeyer H 1997 *Phys. Rev.* B **56** 15 459
[16] Ammer Ch, Meinel K, Wolter H and Neddermeyer H 1998 *Surf. Sci.* **401** 138
[17] Wolter H, Meinel K, Ammer Ch, Wandelt K and Neddermeyer H 1997 *Surf. Sci.* **377–379** 983
[18] Wolter H 1994 *PhD Thesis* Universität Bonn
[19] Berghaus Th, Brodde A, Neddermeyer H and Tosch St 1987 *Surf. Sci.* **184** 273
[20] Kalki K, Wang H, Lohmeier M, Schick M, Milun M and Wandelt K 1992 *Surf. Sci.* **269/270** 310
[21] Meinel K, Wolter H, Ammer Ch, Beckmann A and Neddermeyer H 1997 *J. Phys.: Condens. Matter* **9** 4611
[22] Madey T E, Engelhardt H A and Menzel D 1975 *Surf. Sci.* **48** 393
[23] Ruebush S D, Couch R E, Thevuthasan S, Wang Z and Fadley C S 1997 *Surf. Sci.* **387** L1041
[24] Meinel K, Wolter H, Ammer Ch and Neddermeyer H 1998 *Surf. Sci.* **402–404** 299
[25] Li Yinggang and De Pristo A E 1994 *Surf. Sci.* **319** 141
[26] Meyer G, Wollschläger J and Henzler M 1990 *Surf. Sci.* **231** 64
[27] Meinel K, Wolter H, Ammer Ch, Sebastian I, Beckmann A and Neddermeyer H *Surf. Sci.* at press
[28] Coulman D J, Winterlin J, Behm R J and Ertl G 1990 *Phys. Rev. Lett.* **64** 1761
[29] Jensen F, Besenbacher F, Laegsgaard E and Steensgaard I 1991 *Surf. Sci. Lett.* **259** L774